

Supporting Information

Integrating *in situ* formation of nanozyme with mesoporous polydopamine for combined chemo, photothermal and hypoxia-overcoming photodynamic therapy

Xiaochun Hu^{#a}, Yonglin Lu^{#a}, Xiaoke Shi^a, Tianming Yao^a, Chunyan Dong^{a*}, Shuo Shi^{a*}

^a Shanghai Key Lab of Chemical Assessment and Sustainability, School of Chemical Science and Engineering, Shanghai East Hospital, Tongji University, 1239 Siping Road, 200092 Shanghai, P.R. China.

[#] Contribute equally to this work

E-mail: shishuo@tongji.edu.cn, cy_dong@tongji.edu.cn

Experiments

Materials

Doxorubicin (DOX), 1,3,5-trimethylbenzene (TMB, AR, 97%), tris (hydroxymethyl) aminomethane (Tris, 99.9%), dopamine hydrochloride (98%, AR), chloroplatinic acid (H_2PtCl_6) were purchased from Aladdin Industrial Co., Ltd. (Shanghai, China). Chlorin e6 (Ce6) and bovine serum albumin (BSA) were purchased from Heowns (Tianjing, China). Fetal bovine serum (FBS), phosphate-buffered saline (PBS), Dulbecco's modified Eagle medium (DMEM), penicillin streptomycin solution, and trypsin were ordered from Kai Ji (Nanjing, China). Unless otherwise noted, all chemicals were used without further purification.

Characterizations

Scanning electron microscopy (SEM) was carried out on a Hitachi S-4800 scanning electron microscope. Powder X-ray diffraction was recorded with a Bruker D8 VENTURE X-ray diffractometer with Cu $\text{K}\alpha$ radiation source. Transmission electron microscopic (TEM) images were obtained with a TEOL JEM-2100 transmission electron microscope. Confocal fluorescence imaging was performed on a laser confocal scanning microscope (Leica TCS SP5). Absorption spectra was obtained by a UV-vis (ultraviolet-visible) spectrophotometer (Hitachi U-3900). The 650 nm and 808 nm NIR laser (Changchun Laser) were used to carry out the PDT and PTT study. The camera (DALI TECHNOLOGY) was utilized to monitor the photothermal conversion.

Synthesis of MPDA

The MPDA NPs were prepared referring to the previously reported method. Briefly, 0.54 g of F127 and 0.63 mL of TMB were added into the mixture of H_2O (97.5 mL) and ethanol (90.0 mL) under sonication for 5 min, after that the mixture was kept for further 30 min under drastic agitation. And then, 10 mL tris-solution (9 mg/mL) was added into the mixture, meanwhile, 60 mg of dopamine was also added. The mixture was stirred for 24 h at room temperature. The products were collected by centrifugation (10000 rpm, 15 min), and the template was removed by extraction method, where the products were suspended in a mixed solution (ethanol: acetone, 2:1 v/v) with sonication. The as-prepared MPDA was kept in ethanol for further use.

Synthesis of MPDA-Pt (M-Pt)

H_2PtCl_6 (11.6 mM, 1 mL) was added into MPDA solution (2.5 mg/mL, 8mL) for 1 h. Next, 0.8 mL NaBH_4 (4 mg/mL) was added dropwise under ice bath in 5 min, after that the mixture was stirred for 3 h at room temperature. The

Pt decorated MPDA (M-Pt) was collected by centrifugation (12000 rpm, 10min) and washed with water for several times.

Synthesis of MPDA-Pt-BSA/Ce6/DOX (M-Pt-BCD)

First, the DOX solution (1 mg/mL in PBS, pH=7.4, 15 mL) was mixed the Ce6 solution (1 mg/mL in PBS, pH=7.4, 15 mL). And then, 15 mg MPDA was added into the above solution under stirring for 4 h at room temperature, followed by the addition of 15 mg BSA. After another stirring for 20 h, the DOX and Ce6 co-loaded nanoparticles were collected by centrifugation (12000 rpm, 10 min) and washed with PBS to remove the unloaded components. The loading capacity (LC) and loading efficiency (LE) of DOX and Ce6 were evaluated as follows:

$$LC (\%) = (M_{\text{total DOX or Ce6}} - M_{\text{DOX or Ce6 in supernatant}}) / M_{\text{M-Pt-BCD}} * 100$$

For the preparation of MPDA-Pt-BSA/Ce6 (M-Pt-BC), all the procedures were similar to that M-Pt-BCD except with no addition of DOX.

The Catalase-like activity of M-Pt-BCD

The same concentration of H₂O₂ (120 mM) was incubated with 20 µg/mL M-Pt-BCD or 20 µg/mL M-BCD under stirring, and the mixture volume was 5 mL. The real-time production of oxygen was acquired by an oxygen dissolving instrument.

Cellular uptake

Flow cytometry (BD FACS Aria II, USA) and confocal laser scanning microscopy (Nikon A1R) was employed to study the cellular uptake behaviours of M-Pt-BCD in breast cancer cells (MDA-MB-231). Cells were cultured in 6-well plates (~ 10 × 10⁴ cells per well) for 24 h. After that, 5 µg/mL of M-Pt-BCD was added, meanwhile, for the control group, equal concentration of Ce6 was added. The cells were harvested and washed with ice-cold PBS after 2 h incubation. The fluorescence of Ce6 in cells was measured through flow cytometry.

To determine the location of M-Pt-BCD NPs in cells, MDA-MB-231 cells were seeded in glass culture dishes (35 mm diameter), and followed counterstaining with M-Pt-BCD (5 µg/mL, 2h) and Hoechst 33342 (5 µg/mL, 30 min). The cells were washed repeatedly with PBS and observed by a confocal microscope.

***In vitro* singlet oxygen (¹O₂) generation**

The DCFH was employed as an indicator for the detection of ¹O₂. Briefly, 10 µL of DCFH solution (2 mM) was mixed with 10 µg/mL of M-Pt-BCD dispersion (1mL). For hypoxia conditions, before proceeding the test, the mixture was ventilated with N₂ for 30 min to remove the dissolved oxygen. Afterward, 10 µL of H₂O₂ (10 mM) was added. Then the mixture was exposed to 650 nm irradiation (40 mW/cm²), and the increase of DCFH fluorescence was measured by the FL spectrophotometer. And the generation of ¹O₂ was related with the increase of the fluorescence intensity of DCFH linearly. The experiments of control groups (M-BCD and H₂O₂-blank) were conducted with same steps.

Furthermore, DCFH-DA was used as a probe for the intracellular ROS production. In a typical process, after incubating with MDA-MB-231 cells with M-Pt-BCD (10 µg/mL) for 4 h, the cell culture was changed to the fresh media containing 10 µM DCFH-DA, and followed by incubating for another 20 min. Then, the cells were illuminated under a 650 nm laser (40 mW/cm²) for 5 min before observation by confocal microscope (Ex=488 nm, Em=500-550 nm).

***In vitro* photothermal performance**

The photothermal performance of M-Pt-BCD *in vitro* was studied by recording the temperature changes of M-Pt-BCD aqueous dispersions (0, 25, 50, 100, 200 µg/mL) under 808 nm laser irradiation (0.3, 0.6, 0.9, 1.2 W/cm²) for 5 min. The infrared thermal (IRT) images were also collected by IR thermal camera at selected time points.

***In vitro* the synergic therapeutic efficacy**

To investigate the enhanced PDT efficiency via the catalase-like of Pt, the cytotoxicity against MDA-MB-231 cells was measured by CCK-8 assay under normoxia and hypoxia conditions. For hypoxic photocytotoxicity experiments, the 96-well plates were kept under hypoxia condition for 1 h, and then irradiated with 650 nm laser (40 mW/cm²) under airproof for 5 min. For the *in vitro* synergetic therapy, MDA-MB-231 cells (10⁴ cells per well, 96-well plate) were incubated with M-Pt-BCD, M-Pt-BCD + 650 nm laser, M-Pt-BCD + 808 nm laser, and M-Pt-BCD + 650/808 nm laser, respectively. Finally, the cells viability was measured by CCK-8 assay.

***In vivo* fluorescence and photothermal imaging**

All experiments *in vivo* were conducted in compliance with the guidelines of the Ethics Committee of Shanghai East Hospital (Shanghai, China). Tumour xenograft model was established by breast fat pad orthotopic transplantation on the BALB/c nude mice (5-6 weeks old, female, ~20 g). 5 × 10⁵ MDA-MB-231 cells were injected into the right mammary fat pad for each mouse. After tumour volume reached 200-300 mm³, the fluorescent imaging was performed by Night OWL LB 983 IN VIVO imaging system. Mice injected with Ce6 (100 µL, 1.75 mg/mL), M-Pt-BCD (100 µL, 5 mg/mL) were observed at 1 h, 3 h, 12 h and 24 h. Finally, all mice were sacrificed to excise main organs (heart, lung, liver, spleen and kidney) and the tumours for further observation.

For *in vivo* photothermal effect evaluation, tumour-bearing mice were administrated with 100 µL of 5 mg/mL M-Pt-BCD, and then irradiated with 808 nm NIR laser at the power density of 0.6 W/cm² for 5 min at 24 h post intravenous injection. The tumour temperatures of mice were also recorded with the IR camera thermographic system. The tumour-bearing mice injected with PBS were selected as the control.

***In vivo* antitumor efficiency evaluation**

When the average tumour volume approached 50 mm³, the tumour-bearing mice were randomly divided into 7 groups (n = 5): (1) PBS, (2) M-Pt-BC, (3) free DOX only, (4) M-Pt-BCD, (5) M-Pt-BCD 650 nm laser, (6) M-Pt-BCD 808 nm laser, (7) M-Pt-BCD 650 + 808 nm laser. Intravenous injection of M-Pt-BC or M-Pt-BCD suspension was conducted at a 2-day interval (5 mg/Kg). The tumour sites were illuminated with near-infrared laser post injection for 24 h (808 nm laser: 0.6 W/cm², 10 min; 650 nm laser: 40 mW/cm², 10 min). Tumour sizes and mice body weight were recorded every 2 days. Tumour weight was measured after all mice were sacrificed on day 15. Tumour volume was calculated using the following formula:

$$\text{Tumour volume} = (\text{length} \times \text{width} \times \text{width}) / 2$$

Statistical analysis

One-way single factorial of variance (ANOVA) was performed for all data analysis and values were presented as means ± standard deviation. P < 0.05 (*), P < 0.01 (**), and P < 0.001 (***) mean significant difference. All the data was analyzed by SPSS 19.0.

Abbreviations for nanoparticles

M-Pt-BCD MPDA-Pt-BSA/Ce6/DOX

M-BCD MPDA-BSA/Ce6/DOX

M-Pt-BC MPDA-Pt-BSA/Ce6

M-BC MPDA-BSA/Ce6
M-BD MPDA-BSA/DOX

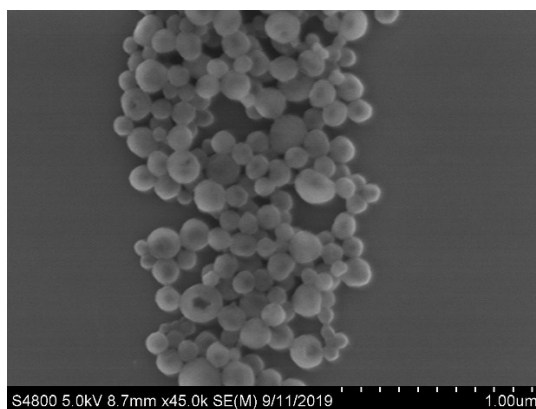


Figure S1. SEM imaging of MPDA.

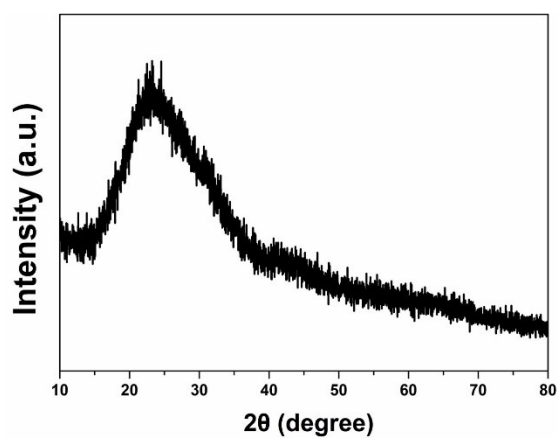


Figure S2. XRD pattern of the prepared MPDA sample.

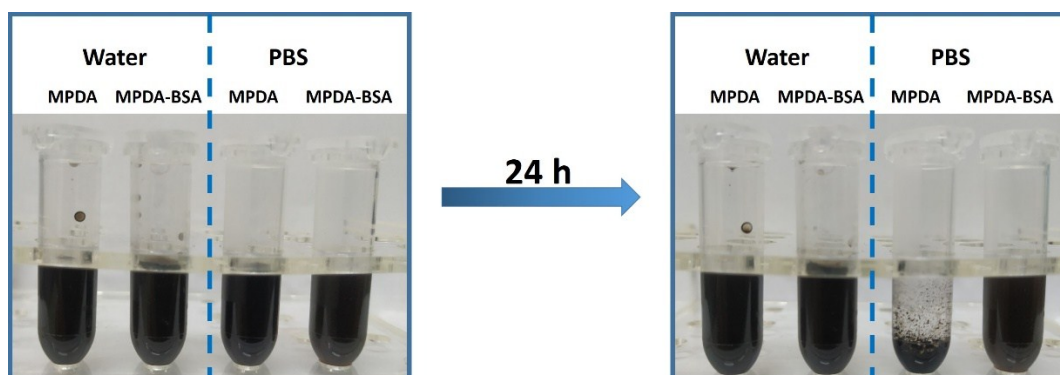


Figure S3. Digital photos of the MPDA and MPDA-BSA in water and PBS.

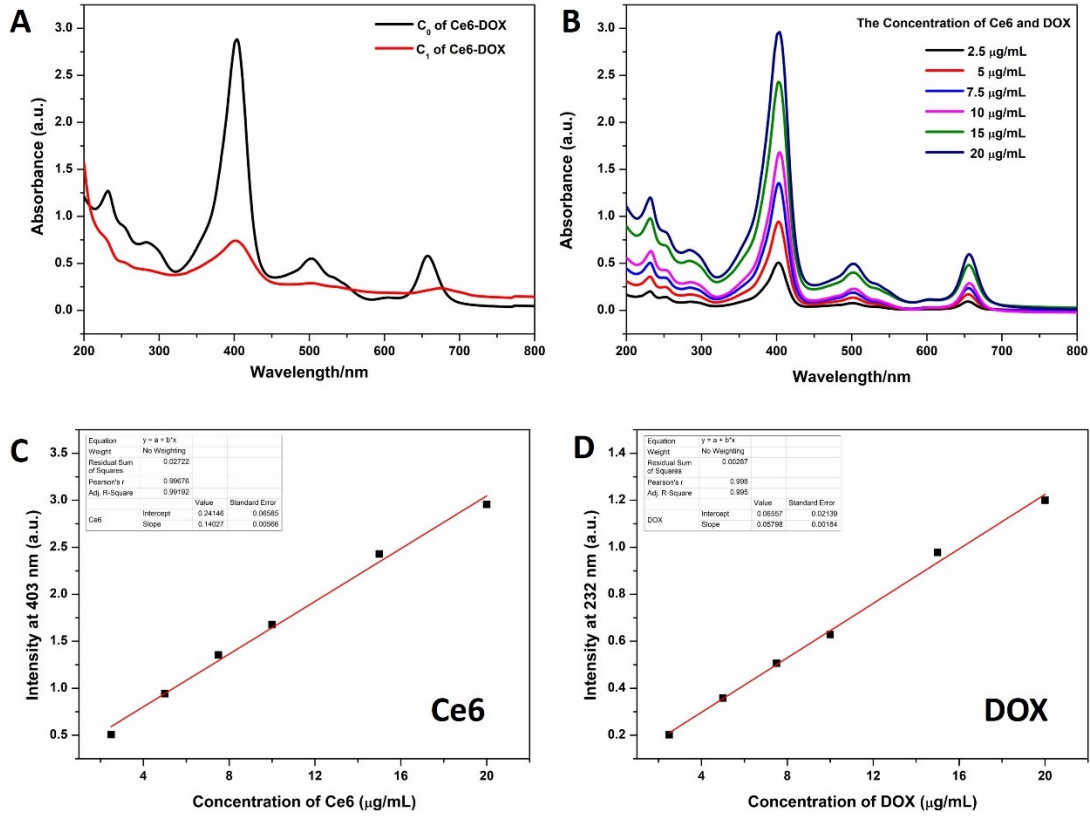


Figure S4. (A) UV-Vis spectroscopy of free Ce6-DOX and supernatant Ce6-DOX after loading. (B) UV-Vis spectra of DOX-Ce6 mixture at various concentrations. (C) Calibration curve of Ce6 at 403 nm. (D) Calibration curve of DOX at 232 nm.

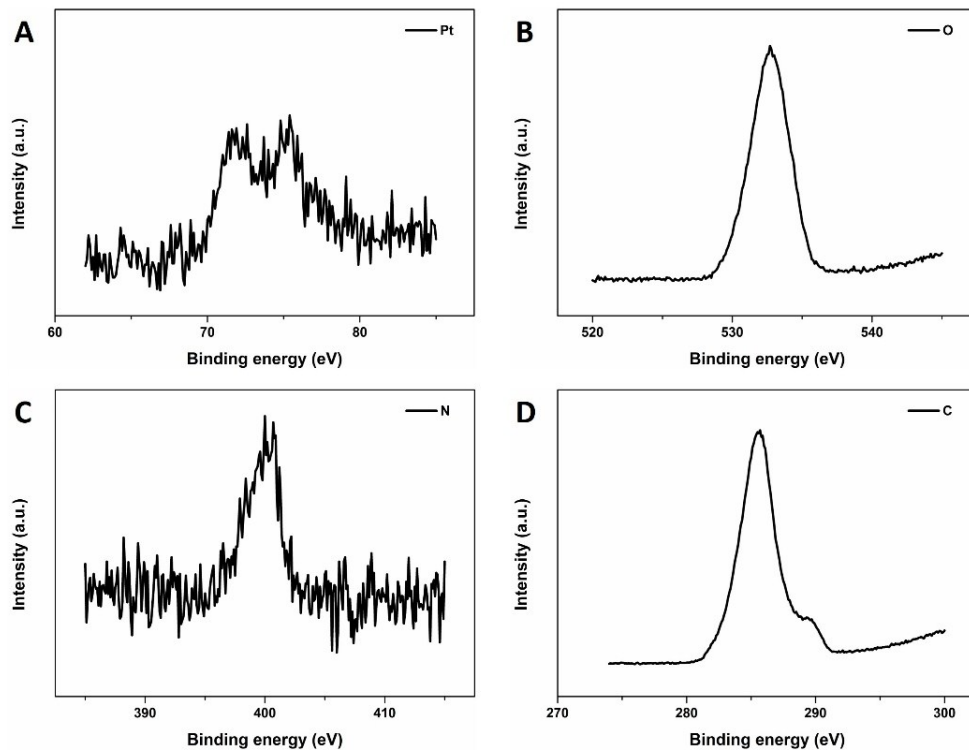


Figure S5. XPS spectra of (A) Pt 4f, (B) O 1s, (C) N 1s and (D) C 1s.

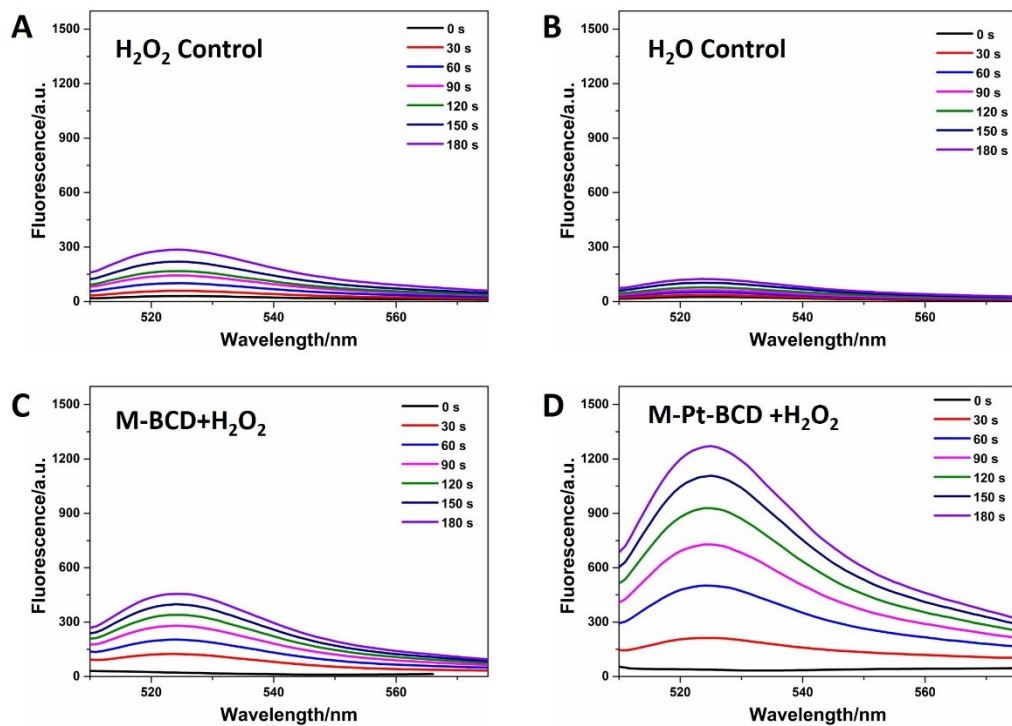


Figure S6. Time-dependent emission spectra of DCFH for (A) H₂O₂ control, (B) H₂O control, (C) M-BCD and (D) M-Pt-BCD upon 650 nm irradiation.

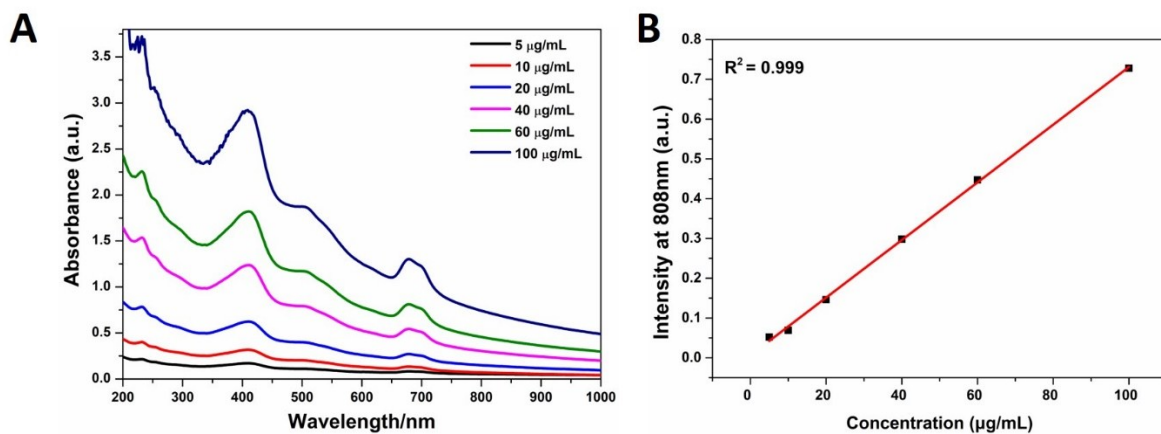


Figure S7. (A) UV-Vis-NIR absorption spectra for aqueous dispersions of M-Pt-BCD NPs with various concentrations. (B) Plots of linear fitting absorbance at 808 nm versus concentration for aqueous dispersions of M-Pt-BCD.

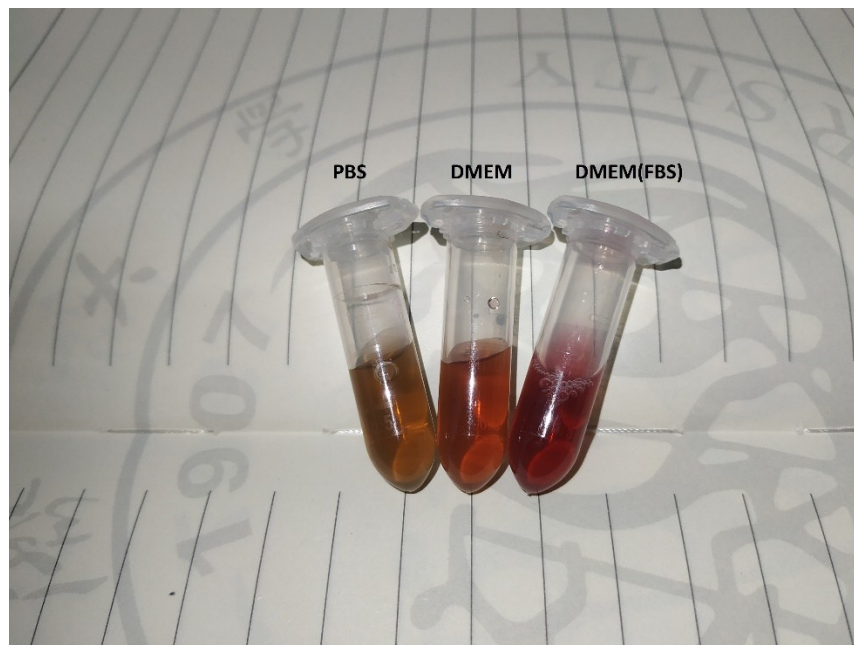


Figure S8. Digital photos of the M-Pt-BCD in PBS, DMEM and DMEM(FBS) (100 $\mu\text{g/mL}$).

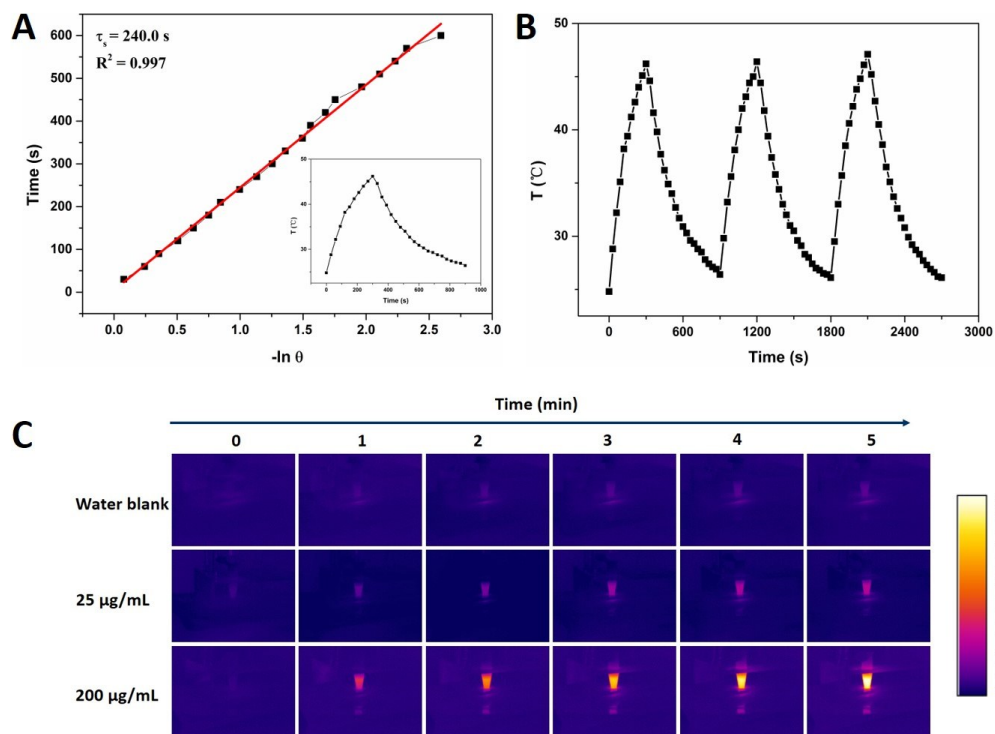


Figure S9. (A) The corresponding linear fitting curve between the plot of cooling time date and $-\ln\theta$. Inset: temperature changes of M-Pt-BCD dispersion irradiated under laser and the cooling stage. (B) Temperature changes of M-Pt-BCD dispersion (100 µg/mL) during three on/off of 808 nm laser irradiation. (C) IRT images during laser irradiation (0.6 W/cm², 5min).

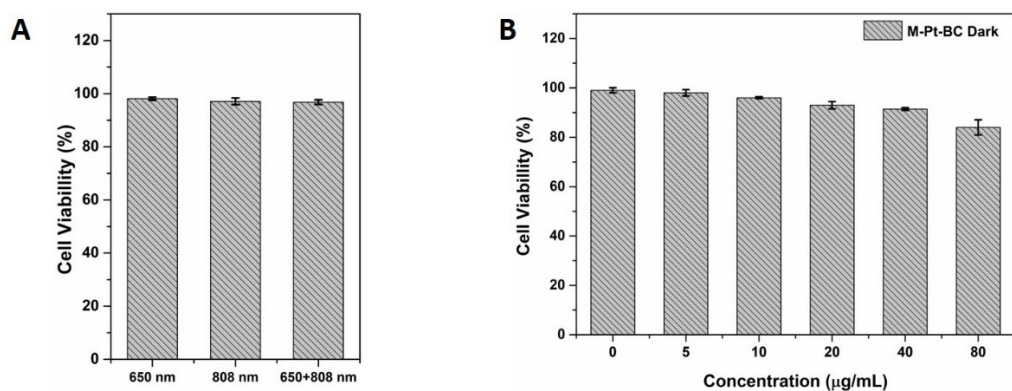


Figure S10. (A) Cell viability of MDA-MB-231 cells upon irradiation alone. (B) Cell viability of MDA-MB-231 cells treated with different concentrations of M-Pt-BC for 48 h under dark.

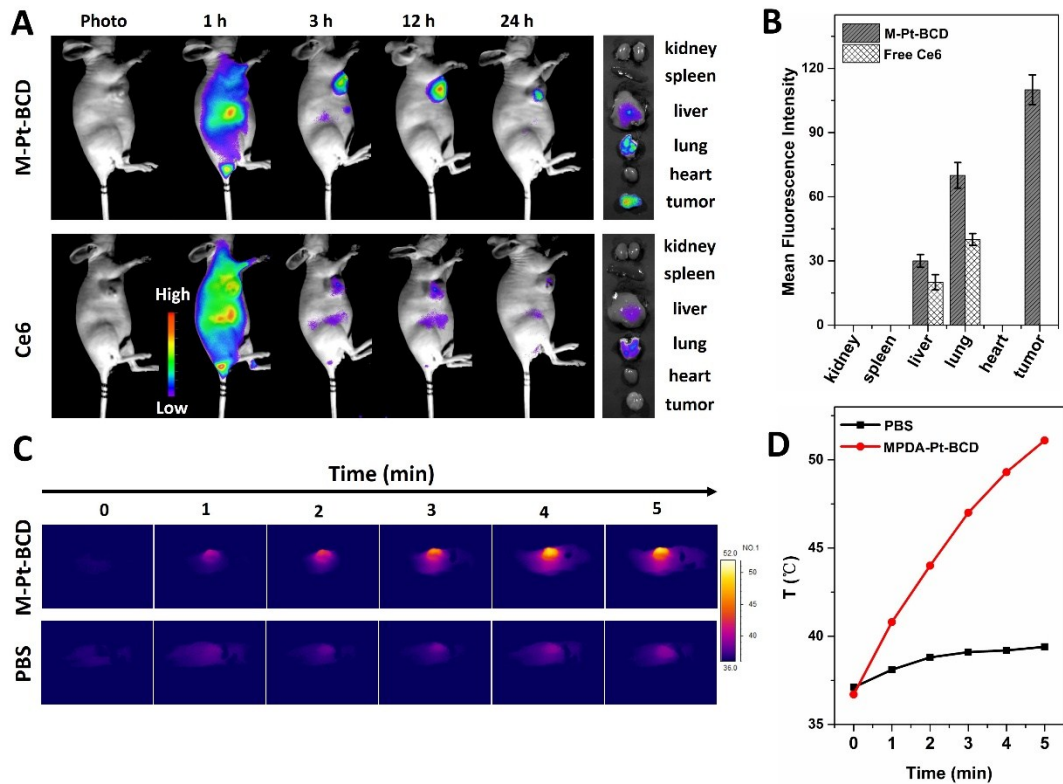


Figure S11. (A) The fluorescence imaging in mice at 1 h, 3 h, 12h and 24 h post injection and main organs and tumours isolated from mice at 24 h post injection of M-Pt-BCD and free Ce6. (B) MFI of main organs and tumours at 24 h post injection. (C) The photothermal imaging in mice administrated with M-Pt-BCD and PBS under 808 nm laser for 5 min (0.6 W/cm^2). (D) Photothermal heating curves obtained for mice injected with PBS and M-Pt-BCD under 808 nm laser for 5 min (0.6 W/cm^2).